International Journal of Nanoelectronics and Materials
Volume 13 (Special Issue) Dec 2020 (235-242)

Benefits of Molybdenum Substitution in $Na_3V_2(PO_4)_3$ Cathode Material for Sodium Ion Batteries: A First Principles Study

Mohamad Firdaus Rosle[1,4], Fadhlul Wafi Badrudin[2], Siti Munirah Hasanaly[1,4], Siti Aminah Mohd Noor[2], Mohamad Fariz Mohamad Taib[3] and Muhd Zu Azhan Yahya[1*]

[1]*Faculty of Defence Science and Technology, Universiti Pertahanan Nasional Malaysia, 57000, Kuala Lumpur, Malaysia.*
[2]*Centre for Defence Foundation Studies, Universiti Pertahanan Nasional Malaysia, 57000 Kuala Lumpur, Malaysia.*
[3]*Faculty of Applied Sciences, Universiti Teknologi MARA, 40450 Shah Alam, Malaysia.*
[4]*Advanced Materials Research Centre (AMREC), SIRIM BERHAD, Kulim Hi-Tech Park, 09000 Kulim Kedah, Malaysia.*

ABSTRACT

The first principles study on the structural and electronic properties of $Na_3V_2(PO_4)_3$ (NVP) was performed using first principles calculation. Results on lattice constant, Mulliken analysis and density of state are discussed in this paper. Overall, lattice parameter calculation obtained using GGA-PBEsol functional is in better agreement with the experimental result. Based on atomic population, Na2 is expected to be sodiated first compared to Na1. From the bond order calculation, it was shown that the P-O bond provided thermal stability and contributed to the long-life cycle of the battery. The Na-O bond showed that the ionic character is essential for ion migration. From the Density of state, the overlapping between O 2p and P 3p orbitals forms a strong bond which supports the bond order result. In this study, the calculated band gap value was 2.06 eV and which then decreased to 0.4 eV upon desodiation. The effect of Molybdenum (Mo) substitution on NVP was also studied using virtual crystal approximation method. The volume of NVP increases with increasing amount of Mo^{6+} substitution which eases the migration of ions and this will be beneficial to the electrochemical performance. Thus, this substituted NVP with Mo ($Na_3V_{2-x}Mo_x(PO_4)_3$) cathode material could be a potential candidate for sodium ion batteries.

Keywords: Cathode material, Density Functional Theory, Electronic Properties, Sodium-Ion Battery, Structural Properties.

1. INTRODUCTION

Lithium ion batteries (LIB) are important energy storage devices that are currently mainly used to power a wide range of portable electronic devices such as mobile phone, laptop, *etc* due to their high volumetric capacity and gravimetric capacity. The advances in LIB technology through various R&D efforts over the years has led to a significant increase in efficiency and capacity of LIB for high power application such as electric vehicle. However, due to high cost, and lithium sources that are less abundant, alternatives to lithium such as sodium ion has been explored to power large scale applications. Sodium is very cheap and is the sixth most abundant element in the Earth's crust. It has similar properties with lithium since they are both members of the same group. Due to this, extensive researches have been carried out to develop Sodium-Ion battery (SIB). $NaFe(Fe[CN_6])_3$ [1], $NaFePO_4$ [2], $NaCoO_2$ [3], and $NaFeSO_4F$ [4] are few examples of sodium-ion battery that has been explored.

NASICON (sodium super ionic conductor)-based SIB, $Na_3M_2(PO_4)_3$ (M=transition metal) has recently caught the attention of many researchers due to the NASICON structure which possess

*Corresponding Author: *mzay@upnm.edu.my*

an open framework in which sodium ions are able to move with ease without obvious changes to the cell volume [5].

In order to enhance the performance, carbon coating and doping are required to improve the electronic conductivity. One of the most prominent and potential NASICON cathode material is the $Na_3V_2(PO_4)_3$ [6,7]. This material has high ionic conductivity and thermal stability. However, its poor electronic conductivity impeded the electrochemical performance of this cathode material. Prior to synthesis, it is essential to conduct material prediction and simulation methods which is an efficient way of doing research as it reduces the trial and error process and saves material cost and research time. The outcome of the prediction will complement the experimental finding. First principles based on Density Functional Theory (DFT) which uses the quantum-mechanical description of electron and nuclei can predict the material properties accurately and also provide information of modification to the material [8]. This method greatly contributes to the field of energy storage particularly for LIB and SIB in the development and understanding of physical and chemical properties, behaviour, and phenomenon at the fundamental level. Badrudin et al. [9] performed first principles study on layered $LiFeSO_4OH$ to elucidate the effect of lithium extraction on the structural and electronic properties. Moreover, the effect of vanadium on the properties of $LiFeSO_4OH$ was also investigated and discussed [10]. Tsevelmaa et al. [11] predicted the $LiFeSO_4F$ magnetic ordering and found it to be consistent with the experimental results. Phadke et al. [12] studied the effect of different group one cation inside Prussian Blue cathode material and analysed the behaviour and capability.

To understand the properties of $Na_3V_2(PO_4)_3$, the structural and electronic properties of NVP and their effects upon desodiation are discussed. Prior to that, geometrical optimization was conducted with few exchange correlational functionals to screen the most accurate result for this material. Density of state (DOS) and Bond order (BO) calculations (Mulliken analysis) were performed to investigate the presence of chemical bonding in the structure. Both results are complementing to each other's. Through Mulliken analysis, new insights into the structural behaviour via bond order can be obtained. This information can provide information on the changes in structural and electrochemical properties. Moreover, BO can be used to monitor the bond covalency inside the material. The band gap before and after desodiation were also calculated and discussed. Aside from fundamental study, the effect of molybdenum substitution on the structure can also be clarified. Based on lattice parameters obtained, the volume of the structure increases with the increasing Mo amount and this will be beneficial to the electrochemical performance.

2. COMPUTATIONAL SETTING

All calculations were performed using the Density Functional Theory (DFT) implemented in the Cambridge Serial Total Energy Package (CASTEP) [13]. The linear density approximation (LDA-CAPZ) [14] and general gradient approximation (GGA) exchange correlational functional was used and treated with Perdew Burke Ernzerhof (PBE) scheme [15]. The DFT method has been proven to be one of the most accurate methods for the computation of the electronic structure of solids [16-18]. All calculations were performed using ultrasoft pseudopotential [19] with a 410 eV cut-off energy, and the K-mesh for the Brillouin Zone sampling was set to 4×4×4 using the Monkhorst Pack mesh technique [20]. Spin polarization was taken into account in the calculation because Vanadium naturally exhibits magnetic properties. The structure of $Na_3V_2(PO_4)_3$ and $NaV_2(PO_4)_3$ displayed in Figure 1 was constructed based on the atom coordinates as shown in Table 1 which was obtained from the experimental data using Material Studio Visualizer [21]. As for $NaV_2(PO_4)_3$, the structure was obtained by removing Na2. For the Molybdenum substitution, virtual crystal approximation (VCA) method was used.

3. RESULTS AND DISCUSSION

Table 2 shows the result of structural parameter of the $Na_3V_2(PO_4)_3$ and $NaV_2(PO_4)_3$ obtained from structural optimisation using GGA-PBE, GGA-PBEsol and LDA exchange correlation functional. For $Na_3V_2(PO_4)_3$ structure, GGA-PBE, and GGA-PBEsol generate overestimated volume and LDA generates underestimated volume. Meanwhile for $NaV_2(PO_4)_3$ structure, all functionals generate overestimated volume. Based on calculation, upon desodiation, about 5.4% (LDA), 6.84% (GGA-PBE) and 8.97% (GGA-PBEsol) volumes have shrunk. Meanwhile, from experiment findings, about 9% of volume has shrunk. This volume shrunk is in consistence with larger radius of Na. Meanwhile, 8.44% volume shrunk has been recorded for lithium-based cathode [22]. Thus, the small volume increment for $NaV_2(PO_4)_3$ structure showed that this cathode material can withstand changes and will be able to provide long cycle of life.

Overall, for both structures, GGA-PBEsol functional showed better agreement with experimental data when compared to GGA-PBE and LDA functional. Based on literatures [23,24,25], it is well known and accepted that GGA-PBE and LDA functional very often overestimate and underestimate the lattice constant calculation. Meanwhile, GGA-PBEsol which is the revised version of PBE always has better agreement with the experimental result [26]. The best method so far is to use the hybrid function (HSE06) which gives the best agreement with the experimental data. Overall, all these calculations are still acceptable. In this present work, GGA-PBEsol calculation are applied as the volume changes are in the closest agreement with the experimental data.

Table 1 The atom coordinate of $Na_3V_2(PO_4)_3$

Elements	***x***	***y***	***z***
Na1	0.63747	0	0.25
Na2	0	0	0
P	0.29683	0	0.25
O1	0.01714	0.20172	0.19119
O2	0.18532	0.16658	0.08488
V	0	0	0.14679

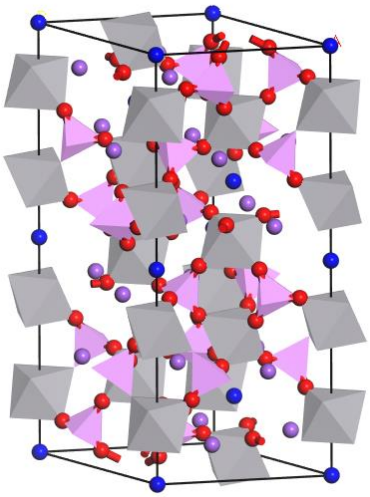

Figure 1. Crystal structure of (a) $Na_3V_2(PO_4)_3$. Blue, purple, pink, red and grey represent Na1, Na2, phosphate, oxygen, and vanadium respectively.

Table 2 Structural parameters of $Na_3V_2(PO_4)_3$ and $NaV_2(PO_4)_3$ from LDA and GGA-PBE compared to experimental data

Structure	Method	*a* =b (Å)	*c* (Å)	V (Å^3)
$Na_3V_2(PO_4)_3$	LDA	8.809 (+1.02%)	20.596 (-5.37%)	1384.01 (-3.43%)
	GGA-PBE	9.005 (+3.27%)	21.345 (-1.93%)	1499.05 (+4.60%)
	GGA-PBEsol	8.929 (2.39%)	21.141 (-2.86%)	1459.66 (+1.85%)
	GGA-PBE [21]	8.938 (2.5%)	22.309 (2.50%)	
	HSE06 [27]	8.719 (-0.01%)	21.422 (-1.57%)	
	GGA-PBE [27]	8.826 (1.79%)	21.634 (-0.59%)	
	Experiment [28]	8.720	21.764	1433.19
$NaV_2(PO_4)_3$	LDA	8.426 (-0.08%)	21.292 (+1.29%)	1309.17 (+1.11%)
	GGA-PBE	8.575 (+1.68%)	21.934 (+4.34%)	1396.67 (+7.87%)
	GGA-PBEsol	8.449 (0.07%)	21.493 (2.25%)	1328.74 (+2.62%)
	GGA-PBE [21]	8.753 (3.79%)	21.846 (3.92%)	
	HSE06 [27]	8.427 (-0.07%	21.304 (1.35%)	
	GGA-PBE [27]	8.557 (1.47%)	21.529 (2.42%)	
	Experiment [28]	8.433	21.021	1294.82

Table 3 shows the atomic population of the atoms in the $Na_3V_2(PO_4)_3$ before and after Na extraction. Na2 is shown to be purely ionic because its charges are near 1+. Meanwhile for Na1, the charge is a bit lower indicating that the significant electrons are shared by neighbouring atom. This showed that there are mix of covalent character between Na1 to neighbouring atom which restricted the Na ion from sodiated. This might be one of the reasons why the Na2 is sodiated first before Na1. Upon desodiation, all the atom charges become more positive. This is due to the movement of electron from cathode to anode in the circuit which accompanies the sodium ion during the extraction. Most of the charges are distributed to V and P atoms. As expected, all the charges do not retain their nominal charges as all the ions inside the cathode material are covalent bonded except for Na ion. Thus, electrons are expected to be shared among them.

Table 3 The atomic population of the atoms in the $Na_3V_2(PO_4)_3$ before and after Na extraction from Mulliken population analysis and their differences in charge Δe

	Sodiated	Desodiated	Δe
Na1	0.65	1.21	0.56
Na2	1.04		1.04
V	0.70	1.22	0.52
P	2.04	2.30	0.26
O1	-0.93	-0.87	0.06
O2	-0.95	-0.89	0.06

Table 4 shows the bond length (BL) and bond order (BO) for $Na_3V_2(PO_4)_3$ and $NaV_2(PO_4)_3$. Based on the result, the overall Na-O bond shows the lowest BO and highest BL values. There are two sets of Na-O bond order values which are 0.12 and 0.09 that belonged to the Na1 site and Na2 site, respectively. Based on this BO value, the Na2 site atom would most likely to be extracted first during the early charging state as the bonding are weaker compared to Na1 site. This is in agreement with the published report [21] and Mulliken population analysis. As for the P-O bond, it has the highest BO and lowest BL values. The higher the BO the more covalent character it possesses and vice versa. The longer the BL, the lower the BO. It this case, Na-O bond displayed the strongest ionic character compared to that of other bonds. This feature is important for application in rechargeable battery as sodium should be able to move freely in the cathode material. The P-O bond is observed to display the strongest covalent character. The presence of PO_4 tetrahedra contributes to high thermal and good structural stability lending the cathode a robust structure to endure repeated cycles of charging and discharging [29]. This function is

similar with other PO_4 based cathode materials such as $LiFePO_4$ [30,31]. Upon desodiation process, only small changes of BL and BO was observed for all bonds. Some of the Na-O bonds also display anti bonding feature (negative BO). Most of the BL and BO values decreased and increased respectively. This showed that the volume of the cathode has contracted slightly.

Table 4 Bond length and bond order (in bracket) for sodiated and desodiated state of $Na_3V_2(PO_4)_3$ and $NaV_2(PO_4)_3$

	Bond Length (Å) (Bond Order)				
Sodiated	**$Na_3V_2(PO_4)_3$**				
Na-O	2.336 (0.12)	2.433 (0.09)	2.444 (-0.04)	2.450 (-0.08)	2.948 (-0.05)
V-O	1.990 (0.35)	2.040 (0.34)			
P-O	1.507 (0.70)	1.522 (0.68)			
Desodiated	**$NaV_2(PO_4)_3$**				
Na-O	2.388 (-0.02)				
V-O	1.886 (0.37)	1.939 (0.34)			
P-O	1.500 (0.67)	1.509 (0.64)			

To further understand the electronic changes upon charge/discharge process and the chemical environment of NVP, the density of state results have been calculated. Figure 2 shows the partial and total density of states (DOS) of (a) $Na_3V_2(PO_4)_3$ and (b) $NaV_2(PO_4)_3$. The calculated value of band gap is about 2.06 eV and 0.4 eV for $Na_3V_2(PO_4)_3$ and $NaV_2(PO_4)_3$ respectively. These values are in agreement with previous published work [30].

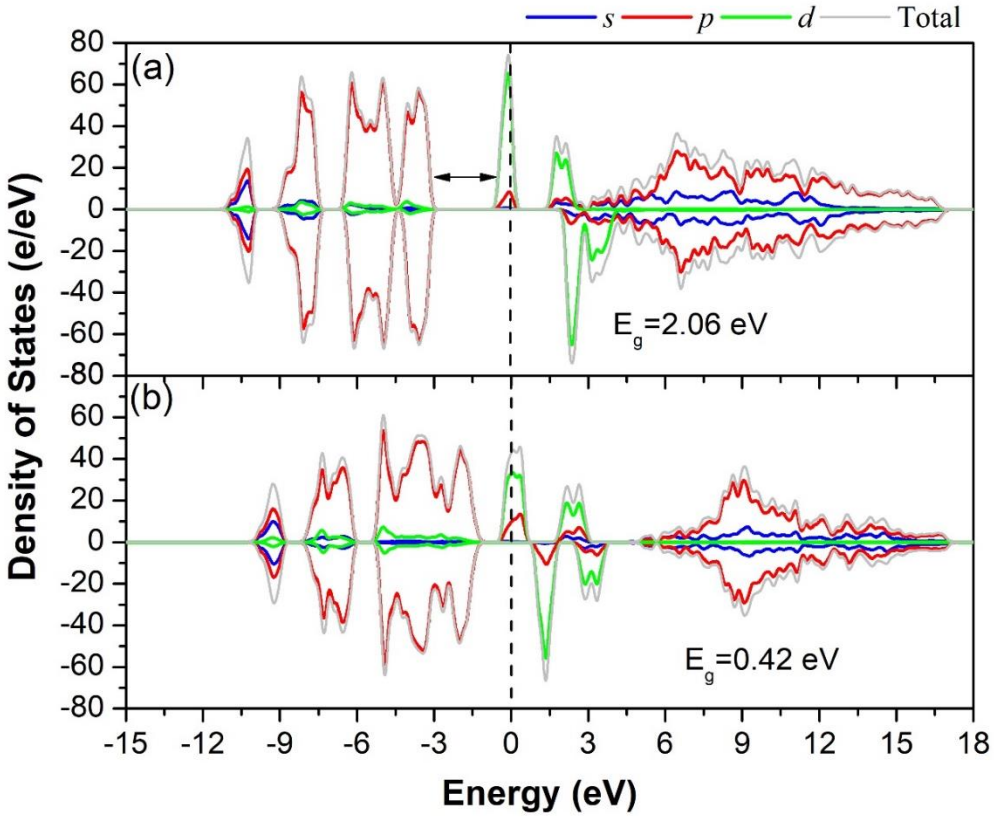

Figure 2. Partial and total density of states (DOS) of $Na_3V2(PO_4)_3$ and $NaV_2(PO_4)_3$.

Upon the extraction of sodium ion, the band gap of $Na_3V_2(PO_4)_3$ decreased which reflects the increased in conductivity. This is due to the oxidation of V^{3+} to V^{4+} as observed in Figure 2 (b) where the V 3d peak shifter from higher to lower energy level. Most of the upper valance band is occupied by O 2p state meanwhile in the lower conduction band, most of it is occupied by V 3d state. In higher conduction band, there are contribution of P 3p and O 2p and both states overlapped forming strong bond. This is in agreement with BO result which shows P-O bond exhibits strong covalent bond which is beneficial to the thermal stability and cycle life of the battery.

To study the effect of Molybdenum substitution NVP, the virtual crystal approximation (VCA) [32] method is performed. In this method the occupancy of the specific atom was changed to simulate the percentage of substitution. By doing this, the crystal is considered as disordered which leads to limitations to the software. Table 5 shows the lattice constant of $Na_3V_{2-x}Mo_x(PO_4)_3$ with the x composition value ranging from 0 to 1. It can be seen that lattice constant *a* and *b* increased with increasing amount of Mo^{+6}. Meanwhile for *c*, the value decreases with increasing amount of Mo^{+6}. This showed that the structure undergoes some degree of distortion. According to Shannon et al. [33], Mo^{6+} and V^{3+} has the ionic radius of 0.55 Å and 0.78 Å, respectively. The substitution site was detected at V^{3+} and since the radius of Mo^{6+} ions are smaller than V^{3+} ions thus distortion is likely to happen. However, the lattice volume did not change in a linear pattern but the insight is still there. The lattice volume decreased initially with the introduction of Mo at a composition of x =0.1 and subsequently increases again with increasing amount of Mo^{6+} ion. This may be due to overestimation of pristine NVP volume calculation. Based on past researches, the lattice volume is found to increase with the increasing Mo^{6+} content [34,35]. This enhances the performance of the battery as an increase in volume will provide extra space for the movement of ions within the cathode thus improving the ionic conductivity.

Based on the past work done by Li et al. [36], they performed the energy migration calculation on NVMoP and found that the energy barrier is reduced compared to the pristine compound and thus, diffusion kinetics of Na ion is improved. Their work also showed that the volume of NVP increased with the increased of Mo^{6+} contents. Similarly, Wang et al. [37] also concluded that sample with Mo doping exhibited better sodium diffusion coefficient as Mo content is good for overcoming kinetics restriction. Meanwhile, for the x=1 concentration the volume of the cell decreased drastically. This speculates that the structure may undergoes a phase change. Previous work by Konishi et al. [38] showed that Mo substitution inside $LiNi_{0.8}Mn_{0.1-x}Co_{0.1}Mo_xO_2$ has induced the phase change from spinel to rock-salt. However, further investigations are required to confirm this speculation.

Table 1 The lattice constant of $Na_3V_{2-x}Mo_x(PO_4)_3$ where x value range from 0 to 1

	a = *b* (Å)	*c* (Å)	V (Å^3)
$Na_3V_2(PO_4)_3$	8.928	21.141	1459.656
$Na_3V_{1.9}Mo_{0.1}(PO_4)_3$	8.915	20.933	1441.070
$Na_3V_{1.7}Mo_{0.3}(PO_4)_3$	8.927	20.883	1441.489
$Na_3V_{1.5}Mo_{0.5}(PO_4)_3$	8.943	20.828	1442.577
$Na_3VMo\ (PO_4)_3$	8.997	20.522	1438.540

4. CONCLUSION

First principles method on $Na_3V_2(PO_4)_3$ was carried out based on density functional theory. Overall, lattice parameters of NVP were best predicted using GGA-PBEsol compared to LDA and GGA-PBE. Both atomic populations result and bond order calculation are in agreement with each other that Na2 will be extracted first upon the initial charging before the Na1. Base on bond order calculation, the Na-O bond has strong ionic character which is important for the movement of

ions inside the cathode material. Meanwhile, the P-O bond contributes to the cycle life and thermal stability as it has strongest covalent bond. This further confirmed by the result of density of state whereby there is an overlapping between P 3p and O 2p orbital to form a strong bonding inside the structure. The calculated band gap for NVP is about 2.06 eV and decreased to 0.4 eV upon desodiation. Molybdenum substitution showed that the conductivity of NVP could be improved with increasing amount of Mo as it expands the volume to create more space for movement of ions. Thus, this substituted NVP with Mo ($Na_3V_{2-x}Mo_x(PO_4)_3$) cathode material could be a potential candidate for sodium ion batteries.

ACKNOWLEDGEMENTS

This work is supported by the Ministry of Higher Education (MOHE) of Malaysia through the Fundamental Research Grant Scheme (Grant code: FRGS/1/2017/STG07/UPNM/01/1). The authors would like to express their gratitude to Institute of Science's Ionic Material Devices (i-MADE) Lab, in Faculty of Applied Science, UiTM for their support in providing research facilities to carry out this research.

REFERENCES

[1] Nasir, N. A. M., Badrudin, F. W., Idrus, A., Sazman, M. F. M. Taib, Yahya, M. Z. A., Mol. Cryst. Liq. Cryst. **693,** 1 (2020) 115–122.
[2] Nakayama, M., Yamada, S., Jalem, R., Kasuga, T., Solid State Ionics. **286** (2016) 40–44.
[3] Samin, N. K., Rusdi, R., Kamarudin, N., Kamarulzaman, N., Adv. Mater. Res. **545** (2012) 185–189.
[4] Barpanda, P., Chotard, J.-N., Recham, N., Delacourt, C., Ati, M., Dupont, L., Armand, M., Tarascon, J.-M., Inorg. Chem. **49,** 16 (2010) 7401–7413.
[5] Zheng, Q., Yi, H., Liu, W., Li, X., Zhang, H., Electrochim. Acta. **238** (2017) 288–297.
[6] Chotard, J. N., Rousse, G., David, R., Mentré, O., Courty, M., Masquelier, C., Chem. Mater. **27**, 17 (2015) 5982–5987.
[7] Q. Zhu, X. Chang, N. Sun, H. Liu, R. Chen, F. Wu, B. Xu, J. Mater. Chem. A. **5**, 20 (2017) 9982–9990.
[8] Meng, Y.S., Arroyo-de Dompablo, M.E., Acc. Chem. Res. **46**, 5 (2013) 1171–1180.
[9] Badrudin, F. W., Taib, M. F. M., Hassan, O. H., Yahya, M. Z. A., Comput. Mater. Sci. **119** (2016) 144–151.
[10] Badrudin, F. W., Taib, M. F. M., Mustapha, R. I. P. R., Hassan, O. H., Yahya, M. Z. A., Mater. Today Proc. **4**, 4 (2017) 5108–5115.
[11] Tsevelmaa, T., Odkhuu, D., Kwon, O., Cheol Hong, S., J. Appl. Phys. **113**, 17 (2013) 17B302.
[12] Phadke, S., Mysyk, R., Anouti, M., J. Energy Chem. **40,** (2019) 31–38.
[13] Segall, Stewart M. D., Pickard, C. J., Hasnip, P. J., Probert, M. I. J., Refson, K., Payne, M. C., Zeitschrift Für Krist. **220** (2005) 567.
[14] Hohenberg, P., Phys. Rev. **136**, 3b (1964) B864–B871.
[15] Perdew, J. P., Burke, K., Ernzerhof, M., Phys. Rev. Lett. **78**, 7 (1997) 1396.
[16] Husin, R., Badrudin, F. W., Taib, M. F. M., Yahya, M. Z. A., Mater. Res. Express. **6**, 11 (2019) 114002.
[17] Yaakob, M. K., Taib, M.F.M., Hassan, O.H., Yahya, M.Z.A., Materials Research Express. vol **2**, (2015) 116101.
[18] Yaakob, M.K., Taib, M. F. M., Deni, M. S. M., Chandra, A., Lu, L., Yahya, M. Z. A., Ceramics International. **39** (2013) S283-286
[19] Vanderbilt, D., Phys. Rev. B. **41**, 11 (1990) 7892–7895.
[20] Monkhorst, H. J., Pack, J. D., Phys. Rev. B. **13**, 12 (1976) 5188–5192.
[21] Song, W., Cao, X., Wu, Z., Chen, J., Huangfu, K., Wang, X., Huang, Y., Ji, X., Phys. Chem. Chem. Phys. **16**, 33 (2014) 17681–17687.

[22] Yin, S. C., Grondey, H., Strobel, P., Anne, M., Nazar, L. F., J. Am. Chem. Soc. 125, 34 (2003) 10402–10411.
[23] Xiao, P., Song, J., Wang, L., Goodenough, J.B., Henkelman, G., Chem. Mater. **27**, 10 (2015) 3763–3768.
[24] Badrudin, F. W., Rasiman, M. S. A., Taib, M. F. M., Hussin, N. H., Hassan, O. H., Yahya, M. Z. A., Adv. Mater. Res. **1107** (2015) 508–513.
[25] He, L., Liu, F., Hautier, G., Oliveira, M. J. T., Marques, M. A. L., Vila, F. D., Rehr, J. J., Rignanese, G. M., Zhou, A., Phys. Rev. B - Condens. Matter Mater. Phys. **89**, 6 (2014) 1–15.
[26] Smith, N. V, Phys. Rev. B. **3**, 6 (1971) 1862–1878.
[27] Bui, K. M., Dinh, V. A., Okada, S., Ohno, T., Phys. Chem. Chem. Phys. **17**, 45 (2015) 30433–30439.
[28] Li, G., Jiang, D., Wang, H., Lan, X., Zhong, H., Jiang, Y., J. Power Sources. **265**, (2014) 325–334.
[29] Lim, S.Y., Kim, H., Shakoor, R.A., Jung, Y., Choi, J.W., J. Electrochem. Soc. **159**, 9 (2012) 1393–1397.
[30] Manthiram, A., Electrochem. Soc. Interface. **18**, 1 (2009) 44–47.
[31] Liu, X., Zhao, Y., Kuang, Q., Li, X., Dong, Y., Jing, Z., Hou, S., Electrochim. Acta. **196**, (2016) 517–526.
[32] Bellaiche, L., Vanderbilt, D., Phys. Rev. B - Condens. Matter Mater. Phys. **61**, 12 (2000) 7877–7882.
[33] Shannon, R. D., Acta Crystallogr. Sect. A. **32**, 5 (1976) 751–767.
[34] Li, X., Huang, Y., Wang, J., Miao, L., Li, Y., Liu, Y., Qiu, Y., Fang, C., Han, J., Huang, Y., J. Mater. Chem. A. **6**, 4 (2018) 1390–1396.
[35] Ding, X., Huang, X., Zhou, S., Xiao, A., Chen, Y., Zuo, C., J. Jin, Int. J. Electrochem. Sci. **14**, 3 (2019) 2815–2821.
[36] Li, X., Huang, Y., Wang, J., Miao, L., Li, Y., Liu, Y., Qiu, Y., Fang, C., Han, J., Huang, Y., J. Mater. Chem. A. **6**, 4 (2018) 1390–1396.
[37] Wang, X., Wang, W., Zhu, B., Qian, F., Fang, Z., Front. Mater. Sci. **12**, 1 (2018) 53–63.
[38] Konishi, H., Yoshikawa, M., Hirano, T., J. Power Sources. **244** (2013) 23–28.